

# On the Performance of the Layered-Division-Multiplexing using Maximal-Ratio Combining

Tanapong Khumyat, Non-member

## ABSTRACT

This article proposes the diversity gain enhancement in layered division multiplexing (LDM) systems by applying maximal-ratio combining (MRC) technique. LDM systems is adopted as a baseline technology of the ATSC 3.0 systems which the two transmission layers are simultaneously transmitted over two different types of fading channels for fixed and mobile services. Hence, the performance analysis of each layer need to be evaluated on different type of fading channel. Starting with the moment generating function (MGF) of the MRC output signal-to-noise ratio (SNR), we propose the new method to derive closed-form expressions for average symbol-error rate (SER) of the proposed systems over Rayleigh and Nakagami- $m$  fading channels in the presence of error propagation (EP) that is generated from the first layer detection. Analytical results show that the specific value of injection level at the transmitter need to be precisely defined to obtain the best mutual benefit for both LDM layers, and the proposed technique has significant performance advantage over conventional LDM systems. Simulation results demonstrate the tightness of the author's analysis

**Keywords:** Layered division multiplexing, Maximal-ratio combining.

## 1. INTRODUCTION

In the next generation digital broadcasting systems and wireless broadband communication systems, the main challenge is to deliver the high data rate multimedia services on the limited frequency resources due to the rapidly increasing demand of the commercial broadband wireless services. The adopted technology should be supported for many required functions to achieve more efficient spectrum utilization and deliver high data rate multimedia services to customers. To facilitate this challenge, the Advance Television Systems Committee (ATSC) call for proposal for the a new international broadcasting standard, called ATSC 3.0, to support high data rate multimedia services in the next generation wireless sys-

tems [1], including mobile HDTV and Ultra HDTV (UHDTV). The key requirement of this standard is to service the high performance transmission including high data rate and large area coverage in low Signal to Noise Ratio (SNR). To enhance this standard, layered division multiplexing (LDM), the Non-Orthogonal Multiplexing (NOM) technique [2], which has been originally proposed as Cloud transmission [3] that support multiple multimedia services in different scenarios including mobile, indoor and stationary channels. Because of advantage and a simple implementation of LDM [4]-[7], a two-layer LDM has been promoted as an optional feature in the ATSC 3.0 physical layer. LDM technique is different from the frequency division multiplexing (FDM) and time division multiplexing (TDM), the multi-layered signals of LDM can be simultaneously transmitted to the receiver by using a single carrier. The two-layer LDM consist of the core layer (CL) stream and the enhanced layer (EL) stream, the higher power CL signal can be directly detected at receiver while the lower power EL signal is acted as additional noise, after that the signal interference cancellation (SIC) receiver is applied to cancel CL stream from the received signal, the EL stream is then detected from the regenerated signal.

The diversity gain and channel capacity of the ATSC 3.0 system can be increased by Multiple-Input Multiple-Output (MIMO) technique [8], [9]. However, due to the complexity of MIMO system in practical detection, the simple technique called Maximal-Ratio Combining (MRC) can be adopted to improve the diversity gain in LDM system [10], [11] instead of MIMO technique. In fact, CL stream is normally encoded by Low-density parity-check (LDPC) codes that offer error free in low SNR region. The EL stream can be then detected without performance degradation by error propagation (EP) in SIC process [6]. However in very low SNR scenario, EP in the EL stream can be occurred at the receiver and the system must take into account the effect of EP in error rate analysis. SER of M-PSK and M-QAM signals with diversity technique over generalized fading channels has been derived by starting with evaluation of the moment generating function (MGF) [13], [14]. To the best of our knowledge, there are no works in literature review that demonstrate the analysis method to acquire a closed-form symbol error rate (SER) ex-

---

Manuscript received on August 20, 2018 ; revised on August 30, 2018.

The author is with Rajamangala University of Technology Lanna Tak, 41 Phaholyothin Rd., Tak, Email: k\_tnp@hotmail.com.

pression for the conventional LDM and MRC-LDM system in the presence of EP [12].

In this paper, the MRC technique is adopted to increase diversity gain of LDM systems. The advantage of the proposed scheme can be demonstrated by analyzing the closed-form error rate performance versus the general LDM systems. The MGF of the MRC output SNR is first evaluated and SER can be then derived for CL stream. Due to the effect of EP, the total probability theorem [9], [15] need to be adopted to calculate the average SER for EL stream. In order to derive SER performance and demonstrate the obvious advantage of MRC-LDM systems, we consider the uncoded MRC-LDM systems without the benefit of LDPC code. The error rate of BPSK signals over Rayleigh fading channel and QPSK signals over Nakagami- $m$  fading channel are analyzed for CL and EL streams, respectively. Numerical results demonstrate the tightness of the author's analysis.

The remainder of this paper is organized as follows. The system and channel models are introduced in the next section while in Section 3, we derive the average bit-error rate (BER) of binary signals over Rayleigh and Nakagami- $m$  fading channels by applying the MGF-based approach. The average SER of M-PSK signals over Nakagami- $m$  fading channels is described in Section 4. In Section 5, the average BER of MRC-LDM system is derived, and numerical examples is also presented. A conclusion of results are given in Section 6.

## 2. SYSTEM AND CHANNEL MODELS

This section presents LDM signal at transmitter and receiver and show the method to derive the SNR per symbol of each receive antenna. Finally, the channel models for the two layers of LDM system are demonstrated.

### 2.1 LDM Signals and Channel Models

At LDM transmitter, the two layers including CL and EL stream are continuously broadcasted over  $L$  independent slowly-varying flat fading channels and transmitted to the MRC-LDM receiver as shown in Fig.1. The LDM complex signal is transmitted over the channel and can be described as

$$s(t) = \sum_{d=-\infty}^{\infty} S^{(d)} e^{-j2\pi f_c t} P(t - dT_s) \quad (1)$$

where  $f_c$  is the carrier frequency, the function  $P(\cdot)$  denotes a pulse shaping waveform of duration  $T_s$  seconds, and  $\{S^{(d)}\}_{d=-\infty}^{\infty}$  denotes the LDM sequence symbols that results from mapping continuous b-bit block into one of  $M = 2^b$  possible waveforms, and can be written as

$$S^{(d)} = S_1^{(d)} + wS_2^{(d)} \quad (2)$$

The LDM signal in (2) is a combined signal including CL stream ( $S_1^{(d)}$ ) and EL stream ( $S_2^{(d)}$ ) that are simultaneously transmitted in different layers have different specifications for the delivery of different services as shown in Fig. 2. The injection level,  $w$  determines the power allocation among the two layers. Meanwhile the higher power of CL stream can be allocated by adjusting the suitable real value  $w$  in  $[0, 1)$ , where  $w=0$  results in a single-layer system. The symbol energy per transmit antenna is assumed equal to  $E_s$ , which the energy  $E_s$  is divided into two portions for CL and EL symbol while the energy ratio for both layers can be adjusted by  $w$ . The energy  $E_p$  and  $w^2 E_p$  are allocated for CL symbol and EL symbol, respectively, where  $E_p = \frac{E_s}{(1+w^2)}$ . From Fig.1, the channel between the transmit antenna and the receive antenna  $i$  is denoted by  $h_i$  where  $h_i = \alpha_i e^{-j\phi_i}$ . The receive signal after passing through the fading channel is disturbed by complex AWGN  $n_i$  with a one-sided power spectral density, which is represented by  $2N_0$  (W/Hz). The received baseband signal on each receive antenna branch is represented by  $r_i$  and can be expressed as

$$\begin{aligned} r_i &= h_i S^{(d)} + n_i \\ &= h_i \left( S_1^{(d)} + wS_2^{(d)} \right) + n_i \end{aligned} \quad (3)$$

In our analysis, the signal combination at MRC receiver will be considered on the MGF of the MRC output SNR in the next part. The first layer CL ( $S_1^{(d)}$ ) can be detected by considering EL signal ( $S_2^{(d)}$ ) as additional noise, thus the detected symbol of CL stream can be acquired from

$$\begin{aligned} \tilde{S}_1^{(d)} &= h_i^{-1} r_i \\ &= S_1^{(d)} + \tilde{n}_i \end{aligned} \quad (4)$$

where  $\tilde{n}_i = wS_2^{(d)} + h_i^{-1} n_i$ . In Appendix 1 we show that the interference-plus-noise energy of  $\tilde{n}_i$  can be expressed as

$$\begin{aligned} E[\tilde{n}_i \tilde{n}_i^*] &= w^2 E_p + N_0 \\ &= w^2 \frac{E_s}{(1+w^2)} + N_0 \end{aligned} \quad (5)$$

where  $E[\cdot]$  is the expectation operator. Based on (4) and (5), the post-processing SNR per symbol of the  $i^{th}$  receive antenna branch for CL stream can be expressed as

$$\tilde{\gamma}_{i,CL} = \frac{\mu \frac{E_s}{N_0}}{(1-\mu) \frac{E_s}{N_0} + 1} \quad (6)$$

where  $\mu = 1/(1+w^2)$ . By considering the process after detecting the CL stream, the EL stream can be then detected by using successive interference cancellation (SIC) to cancel CL signal from the existing

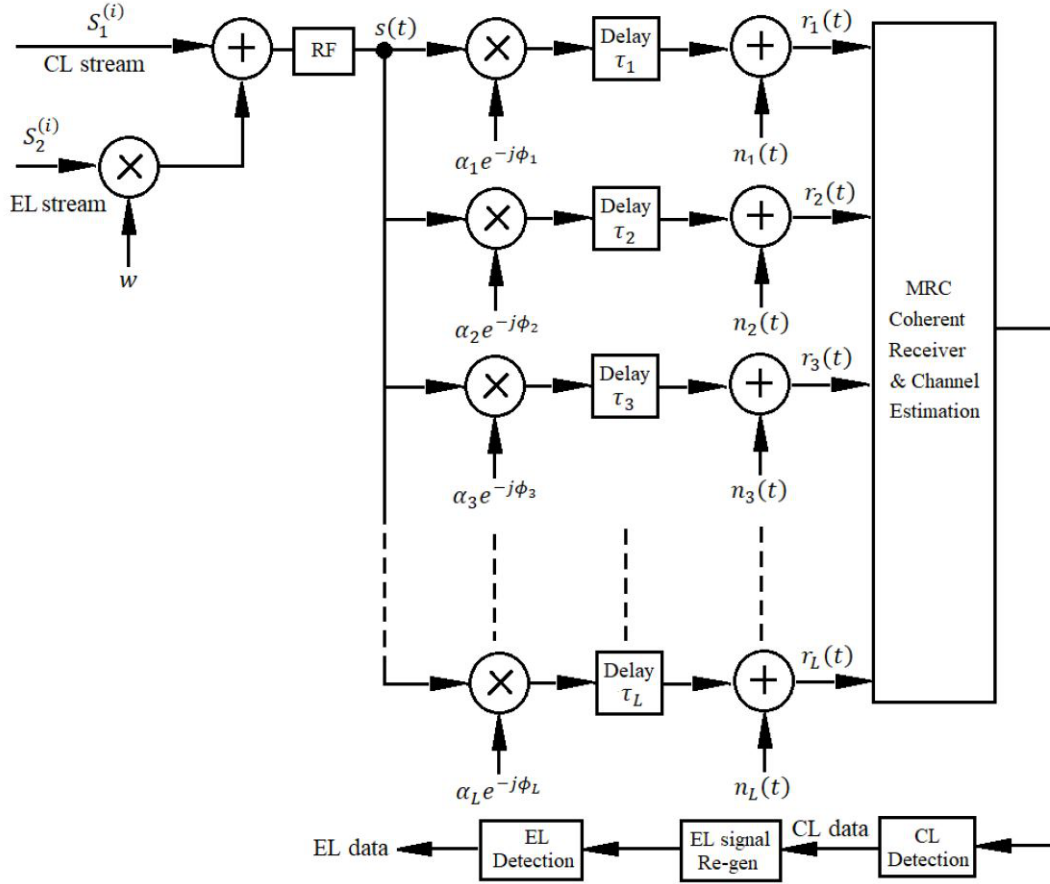


**Fig.1:** Multilink channel model of MRC-LDM systems.

receive signal  $r_i$ , which can be explained by

$$\begin{aligned} r_{i,EL} &= r_i - h_i \hat{S}_1^{(d)} \\ &= h_i (S_1^{(d)} - \hat{S}_1^{(d)}) + h_i w S_2^{(d)} + n_i \end{aligned} \quad (7)$$

where  $r_{i,EL}$  denotes the EL received signal and  $\hat{S}_1^{(d)}$  represents the CL symbol that is chosen from constellation by the maximum likelihood detector (MLD) at the receiver. The results of  $h_i(S_1^{(d)} - \hat{S}_1^{(d)})$  can be divided into two manners, and hence the possible results of the EL received signal is also occurred in two cases as follows

1) *The EL received signal without EP* ( $S_1^{(d)} = \hat{S}_1^{(d)}$ ): This event can be presented when the MLD chooses a correct symbol from constellation, hence there is no EP from the SIC process, then the EL received signal or the regeneration signal can be written as

$$r_{i,EL} = h_i w S_2^{(d)} + n_i \quad (8)$$

The EL signal  $S_2^{(d)}$  can be detected by multiplying (8) with  $h_i^{-1}/w$  as follows

$$\tilde{S}_2^{(d)} = \frac{h_i^{-1}}{w} r_{i,EL} = S_2^{(d)} + \hat{n} \quad (9)$$

where  $\hat{n} = \frac{h_i^{-1}}{w} n_i$ . Based on (9) and the interference-plusnoise energy of  $\hat{n}$  in Appendix 2, the SNR per symbol of each receive antenna branch without EP for EL stream can be expressed as

$$\bar{\gamma}_{ELt} = \frac{w^2 E_p}{N_0} = (1 - \mu) \frac{E_s}{N_0} \quad (10)$$

2) *The EL received signal with EP* ( $S_1^{(d)} \neq \hat{S}_1^{(d)}$ ): This event can be presented when the MLD chooses an incorrect symbol from constellation, hence there is an EP from the SIC process, then the EL received signal or the regeneration signal can be written by

$$r_{i,EL} = h_i w S_2^{(d)} + \Delta_s h_i + n_i \quad (11)$$

where  $\Delta_s$  represents the mean distance of CL symbols pair ( $S_1^{(d)} - \hat{S}_1^{(d)}$ ), which the mean distance can be obtained by averaging the distance of all symbol pairs in constellation. For generalized modulation scheme in LDM system,  $\Delta_s^2 = \rho E_p$ , where the coefficient  $\rho$  is depending on the modulation type ( $\rho = 4$  for BPSK signal). The EL signal  $S_2^{(d)}$  can be detected by multiplying (11) with  $h_i^{-1}/w$  as follows

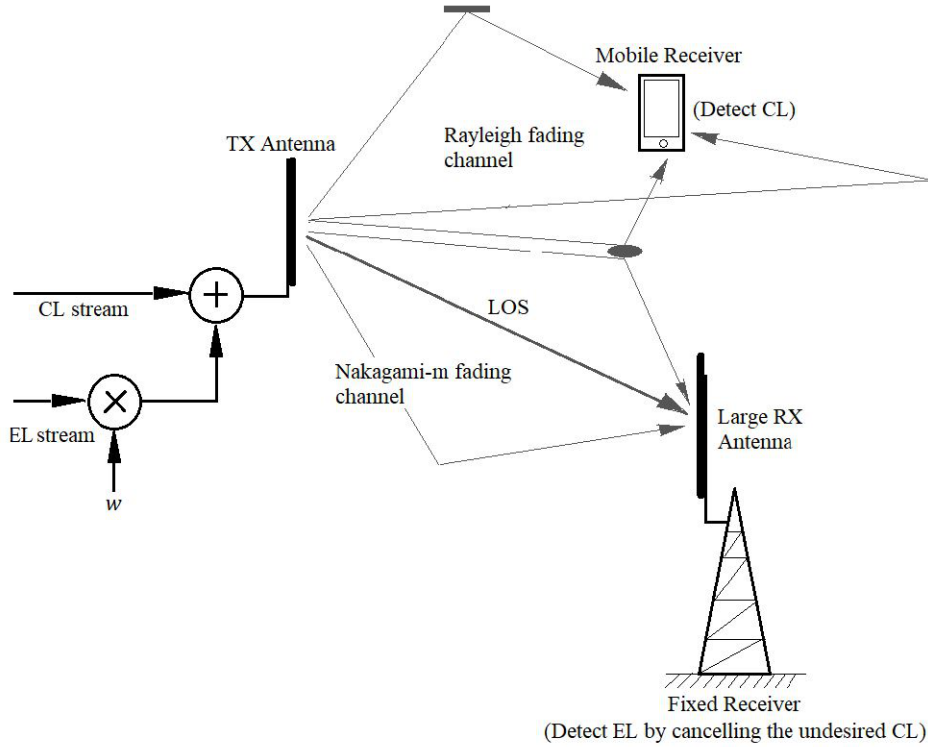


**Fig.2:** Channels of CL and EL layer of LDM systems.

$$\tilde{S}_2^{(d)} = \frac{h_i^{-1}}{w} r_{i,EL} = S_2^{(d)} + n'' \quad (12)$$

where  $n'' = \frac{\Delta_s}{w} + \hat{n}$ . Based on (12) and the interference-plus-noise energy of  $n''$  in Appendix 3, the SNR per symbol of each receive antenna branch with EP for EL stream can be expressed as

$$\bar{\gamma}_{ELf} = \frac{(1 - \mu) \frac{E_s}{N_0}}{\rho \mu \frac{E_s}{N_0} + 1} \quad (13)$$

## 2.2 Channel Models

In the MRC-LDM transmission process, the transmitted signal are passed over independent  $L$  channels where  $l$  denotes the channel index, and the random channel amplitude, phase, and delays are represented by  $\{\alpha_l\}_{l=1}^L$ ,  $\{\phi_l\}_{l=1}^L$  and  $\{\tau_l\}_{l=1}^L$ , respectively. Due to delay of multilink channel, we assume that  $\tau_1 < \tau_2 < \tau_3 < \tau_L$  while  $\tau_1$  is zero for the first channel that is assigned to the reference channel. We define  $\{\alpha_l\}_{l=1}^L$ ,  $\{\phi_l\}_{l=1}^L$  and  $\{\tau_l\}_{l=1}^L$  are all constant over a symbol duration for slow-fading channel in analysis. In general, CL signal is designed to deliver robust mobile broadcasting service to mobile user and indoor receiver. Thus there is only non-line-of-sight (NLOS) path for transmitting CL signal without direct line-of-sight (LOS) path. Therefore the Rayleigh fading channel is assigned to analyze the performance of CL signal transmission as shown in Fig. 2. Meanwhile

EL signal is usually designed to deliver the higher quality service, which usually require higher SNRs for successful detection. The large directional antenna of fixed receiver should be placed at high location that is capable of providing higher SNRs as compared to mobile services [16]. At the fixed receiver, the undesired CL signal is first cancelled and then the EL signal can be detected from the regenerated receive signal. In the transmission link of EL layer, there are two characters of transmission path including direct LOS path and scattered path. Hence the Rician fading channel is an appropriate model to derive the performance of EL signal transmission, while the ratio of signal power in direct LOS path to signal power in scattered path can be assigned by the Rician  $K$ -factor. However the MGF of the received SNR over the Rician fading channel cannot be easily calculated because of integral of the zero<sup>th</sup>-order modified Bessel function. Thus, in order to obtain the MGF by uncomplicated way, this work derives the performance of EL signal transmission over the Nakagami- $m$  fading channel that can be estimated to as the Rician distribution [17], [18], while the relation between the parameter  $K$  and  $m$  of the two channels can be presented as  $m = \frac{K^2 + 2K + 1}{2K + 1}$ . The instantaneous SNR per symbol of the  $l^{th}$  channel  $\gamma_l$  for Rayleigh and Nakagami- $m$  distributions can be referred to as (14) and (15), respectively.

$$p_{\gamma_l}(\gamma_l; \bar{\gamma}_l, r) = \frac{1}{\bar{\gamma}_l} e^{-\frac{\gamma_l}{\bar{\gamma}_l}}, \gamma_l \geq 0 \quad (14)$$

$$p_{\gamma_l}(\gamma_l; \bar{\gamma}_l, m_l) = \frac{m_l^{m_l} \gamma_l^{m_l-1}}{\bar{\gamma}_l^{m_l} \Gamma(m_l)} e^{-\frac{\gamma_l}{\bar{\gamma}_l}}, \gamma_l \geq 0 \quad (15)$$

At the output of MRC combiner, the total conditional SNR per symbol  $\gamma_t$  from  $L$  branches is given by  $\gamma_t = \sum_{l=1}^L \gamma_l$  [13].

### 3. AVERAGE BER OF BINARY SIGNALS

BER of BPSK signal over fading channel for SISO and MRC receiver can be derived by using MGF of Rayleigh and Nakagami- $m$  distribution as follows.

#### 3.1 Average BER for Single-channel Reception ( $L=1$ )

The average BER can be calculated from the conditional BER and envelope probability density function (pdf) as

$$P_b(E) = \int_0^\infty P_b(E|\gamma) p_\gamma(\gamma; \bar{\gamma}, z) d\gamma \quad (16)$$

$$= \frac{1}{\pi} \int_0^{\frac{\pi}{2}} \int_0^\infty e^{-\frac{g\gamma}{\sin^2 \phi}} p_\gamma(\gamma; \bar{\gamma}, z) d\gamma d\phi$$

where  $z$  can be substituted by  $r$  and  $m$  for the Rayleigh and Nakagami- $m$  pdf's, respectively.

1) *Rayleigh fading channel* : From (14) and (16), the average BER over Rayleigh fading channel can be written as

$$P_b(E) = \frac{1}{\pi} \int_0^{\frac{\pi}{2}} \frac{1}{\bar{\gamma}_l} \int_0^\infty e^{-\frac{g\gamma}{\sin^2 \phi}} \cdot e^{-\frac{\gamma}{\bar{\gamma}_l}} d\gamma d\phi \quad (17)$$

By deriving the MGF for Rayleigh distribution in Appendix 4, the average BER from (17) is giving by

$$P_b(E) = \frac{1}{\pi} \int_0^{\frac{\pi}{2}} M_r \left( -\frac{g}{\sin^2 \phi}, \bar{\gamma} \right) d\phi \quad (18)$$

$$= \frac{1}{2} \left( 1 - \sqrt{\frac{g\bar{\gamma}}{1+g\bar{\gamma}}} \right)$$

where (18) can be derived by  $J_N(c) = \frac{1}{\pi} \int_0^{\frac{\pi}{2}} \left( \frac{\sin^2 \phi}{\sin^2 \phi + c} \right)^N d\phi$  [13], [20] for  $N = 1$  and  $c = g\bar{\gamma}$

2) *Nakagami -  $m$  fading channel* : From (15) and (16), the average BER over Nakagami- $m$  fading channel can be written as

$$P_b(E) = \frac{1}{\pi} \int_0^{\frac{\pi}{2}} \int_0^\infty e^{-\frac{g\gamma}{\sin^2 \phi}} \cdot \frac{m^m \gamma^{m-1}}{\bar{\gamma}^m \Gamma(m)} e^{-\frac{\gamma}{\bar{\gamma}}} d\gamma d\phi \quad (19)$$

By deriving the MGF of Nakagami- $m$  distribution in Appendix 5 and function  $J_n(c)$ , the average BER

from (19) is giving by

$$P_b(E) = \frac{1}{\pi} \int_0^{\frac{\pi}{2}} M_m \left( -\frac{g}{\sin^2 \phi}, \bar{\gamma} \right) d\phi$$

$$= \left[ \frac{1}{2} \left( 1 - \sqrt{\frac{g\bar{\gamma}}{1+g\bar{\gamma}}} \right) \right]^m$$

$$\sum_{k=0}^{m-1} \binom{m-1+k}{k} \left[ 1 - \frac{1}{2} \left( 1 - \sqrt{\frac{g\bar{\gamma}}{1+g\bar{\gamma}}} \right) \right]^k \quad (20)$$

The average BER over Nakagami- $m$  fading channel in (20) can be derived by substituting MGF of Nakagami- $m$  distribution in function  $J_N(c)$  and define  $N = m$ .

#### 3.2 Average BER for Multichannel Reception ( $L > 1$ )

When the MRC receiver is used, the multichannel conditional BER  $P_b(E|\{\gamma_l\}_{l=1}^L)$  need to be averaged over the joint pdf of the instantaneous SNR sequence  $p_{\gamma_1, \gamma_2, \dots, \gamma_L}(\gamma_1, \gamma_2, \dots, \gamma_L) = \prod_{l=1}^L p_{\gamma_l}(\gamma_l; \bar{\gamma}_l, m_l)$ , hence the unconditional BER  $P_b(E)$  can be written in general form and MGF form in (21) and (22), respectively [13].

$$P_b(E) = \int_0^\infty \int_0^\infty \dots \int_0^\infty \frac{1}{\pi} \int_0^{\frac{\pi}{2}} \prod_{l=1}^L e^{-\frac{g\gamma_l}{\sin^2 \phi}} \cdot p_{\gamma_l}(\gamma_l; \bar{\gamma}_l, m_l) d\phi d\gamma_1 d\gamma_2 \dots d\gamma_L \quad (21)$$

$$P_b(E) = \frac{1}{\pi} \int_0^{\frac{\pi}{2}} \left( M_i \left( -\frac{g}{\sin^2 \phi}, \bar{\gamma} \right) \right)^L d\phi \quad (22)$$

where all fading paths in (21) are uniformly distributed with the same fading parameter  $i$  and the same average SNR per bit  $\bar{\gamma}$  for all  $L$  channels. Hence, the simple form of average BER can be demonstrated as in (22).

1) *Rayleigh fading channel* : By considering the MGF for Rayleigh distribution [13] and the function  $J_N(c)$ , the average BER of MRC receiver from (22) can be expressed as

$$P_b(E) = \frac{1}{\pi} \int_0^{\frac{\pi}{2}} \left( M_i \left( -\frac{g}{\sin^2 \phi}, \bar{\gamma} \right) \right)^L d\phi$$

$$= \left[ \frac{1}{2} \left( 1 - \sqrt{\frac{g\bar{\gamma}}{1+g\bar{\gamma}}} \right) \right]^L$$

$$\sum_{k=0}^{L-1} \binom{L-1+k}{k} \left[ 1 - \frac{1}{2} \left( 1 - \sqrt{\frac{g\bar{\gamma}}{1+g\bar{\gamma}}} \right) \right]^k \quad (23)$$

2) *Nakagami -  $m$  fading channel* : By considering

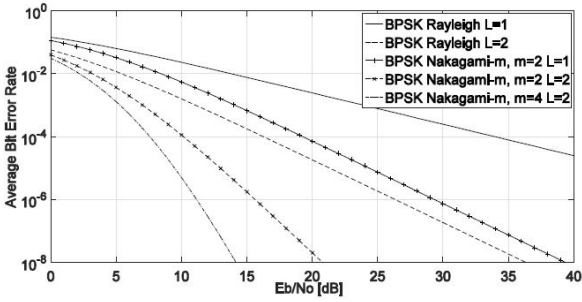


**Fig.3:** BER performance comparison between BPSK SISO receiver, and BPSK MRC receive ( $L = 2$ ) with  $m = 1$ ,  $m = 2$  and  $m = 4$ .

the MGF for Rayleigh distribution [13] and the function  $J_N(c)$ , the average BER of MRC receiver from (22) can be expressed as

$$\begin{aligned} Pb(E) &= \frac{1}{\pi} \int_0^{\frac{\pi}{2}} \left( M_m \left( -\frac{g}{\sin^2 \phi}, \bar{\gamma} \right) \right)^L d\phi \\ &= \left[ \frac{1}{2} \left( 1 - \sqrt{\frac{g\bar{\gamma}}{1 + \frac{g\bar{\gamma}}{m}}} \right) \right]^{mL} \\ &\quad \sum_{k=0}^{mL-1} \binom{mL-1+k}{k} \left[ 1 - \frac{1}{2} \left( 1 - \sqrt{\frac{g\bar{\gamma}}{1 + \frac{g\bar{\gamma}}{m}}} \right) \right]^k \end{aligned} \quad (24)$$

### 3.3 Numerical Example

Fig. 3 shows the effect of  $L$  and  $m$  on the average error rate of BPSK. The BER performance of SISO and SIMOMRC over Rayleigh fading and Nakagami- $m$  fading can be derived by applying (18), (20), (23), and (24). These curves confirm the benefit of MRC receiver, a diversity gain and BER performance of wireless link can be significantly improved by increasing the number of  $L$  at MRC receiver of the LDM systems. Moreover, the BER performances are varied according to the characteristic of channels when varying  $m$  parameter.

### 4. AVERAGE SER OF $M$ -PSK SIGNALS

By considering EL signal transmission in this work, the transmitted QPSK signal is broadcasted over Nakagami- $m$  fading channel and accepted by the fixed MRC receiver. Thus the average SER for this scenario can be expressed as [13]

$$BER_{CL} = \left[ \frac{1}{2} \left( 1 - \sqrt{\frac{g \frac{\mu \frac{E_s}{N_0}}{(1-\mu) \frac{E_s}{N_0} + 1}}{1 + g \frac{\mu \frac{E_s}{N_0}}{(1-\mu) \frac{E_s}{N_0} + 1}}} \right) \right]^{L-1} \sum_{k=0}^{L-1} \binom{L-1+k}{k} \left[ 1 - \frac{1}{2} \left( 1 - \sqrt{\frac{\frac{\mu \frac{E_s}{N_0}}{(1-\mu) \frac{E_s}{N_0} + 1}}{1 + g \frac{\mu \frac{E_s}{N_0}}{(1-\mu) \frac{E_s}{N_0} + 1}}} \right) \right]^k \quad (27)$$

$$\begin{aligned} P_s(E) &= \frac{1}{\pi} \int_0^{\left(\frac{M-1}{M}\right)\pi} \prod_{l=1}^L M_m \left( -\frac{gPSK}{\sin^2 \phi}, \bar{\gamma} \right) d\phi \\ &= \frac{1}{\pi} \int_0^{\left(\frac{M-1}{M}\right)\pi} \left( \frac{\sin^2 \phi}{\sin^2 \phi + \frac{gPSK\bar{\gamma}}{m}} \right)^{mL} d\phi \\ &= \frac{1}{\pi} \int_0^{\left(\frac{M-1}{M}\right)\pi} \left( \frac{\sin^2 \phi}{\sin^2 \phi + \hat{a}\bar{\gamma}} \right)^{mL-1} \left( \frac{\sin^2 \phi}{\sin^2 \phi + \hat{a}\bar{\gamma}} \right) d\phi \end{aligned} \quad (25)$$

where  $gPSK = \sin^2(\phi/M)$ ,  $M = 4$  for QPSK signal and  $\hat{a} = \frac{gPSK}{m}$ . Then (25) can be transformed to the integral of a trigonometric function  $I_{n+1}(\theta; c)$  [14] as

$$P_s(E) = I_{mL} \left( \left( \frac{M-1}{M} \right) \pi; \hat{a}\bar{\gamma} \right) \quad (26)$$

### 5. AVERAGE BER OF MRC-LDM SYSTEMS

Generally, the LDM detection process can be demonstrated in Fig.2, the receiver of mobile user detect CL stream by considering the low power EL stream as an additional noise [7]. Meanwhile the receiver of fixed user detect the undesired CL stream first by considering the low power EL stream as an additional noise. Then the undesired CL stream is cancelled from received signal of the fixed user and the EL stream can be subsequently detected in the presence of EP. Thus, to analyze the average BER of the CL and EL signals at MRC receiver, we should consider the level of EL signal that is controlled by injection level  $w$ , and assign the number of receive branches  $L$  appropriately.

#### 5.1 Average BER of CL Stream

To derive BER performance of BPSK signal over Rayleigh fading channel at the mobile receiver, the postprocessing SNR per symbol of the CL stream in (6) can be substituted into (23) to derive the average BER of the CL signal as (see (27))

For case of undesired CL stream at a fixed receiver, the  $BER_{CL'}$  of BPSK and MPSK signal over Nakagami- $m$  fading channel can be derived by substituting (6) into (24) and (26), respectively.

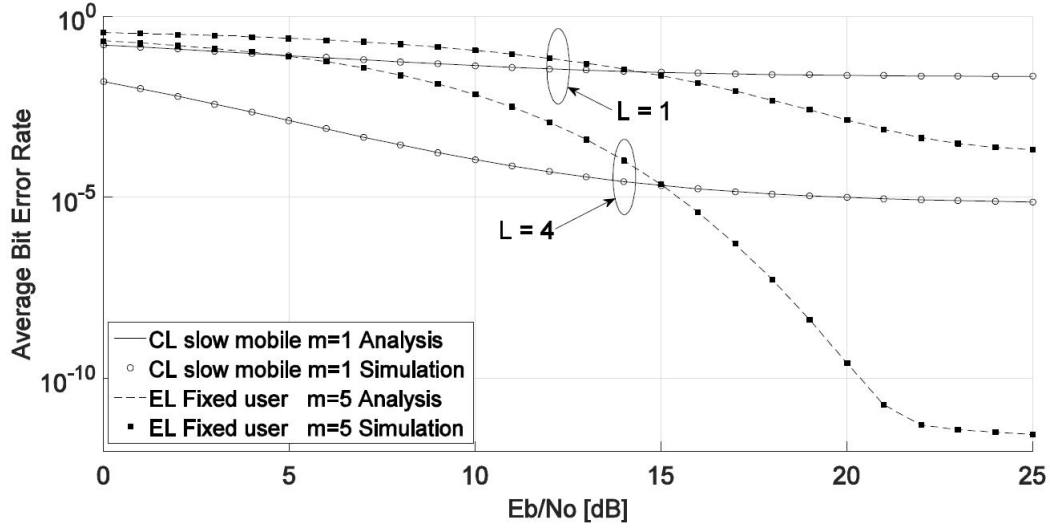


**Fig.4:** BER advantage of MRC-LDM ( $L = 4$ ) over SISO-LDM ( $L=1$ ).

## 5.2 Average BER of EL Stream

In this work, EL and undesired CL streams are mutually transmitted over the Nakagami- $m$  fading channel and accepted by the fixed receiver. The fixed receiver detect the undesired CL stream first and then detect the EL stream after cancelling the undesired CL stream from the existing receive signal which the possible output of cancellation can be divided into two manners. For the first event, the undesired CL signal is correctly detected and the postprocessing SNR per symbol of the EL stream can be derived as in (10). And the second, the undesired CL signal is incorrectly detected and the post-processing SNR per symbol of the EL stream is shown in (13). The two SNRs per symbol of different events are directly affected to the average BER of EL stream. Therefore the total probability theorem can be applied [9], [15] to derive the average BER of EL stream by substituting (10) and (13) into (26) as follows. (see (28))

where  $BER_{CL'}$  denotes the average BER of unde-

sired CL signal that is evaluated over the Nakagami- $m$  fading channel at the fixed receiver while the post-processing SNR per symbol of the CL stream in (6) can be substituted into (24),  $P_s(E, \bar{\gamma}_{ELf})$  denotes the average SER in (26) that substituting by  $\gamma_{ELf}$  from (13),  $P_s(E, \bar{\gamma}_{ELt})$  denotes the average SER in (26) that substituting by  $\gamma_{ELt}$  from (10) while the modulation method can be chosen by varying  $M$ , and

$$\delta = \frac{1}{2} \left( 1 - \sqrt{\frac{g\tilde{\gamma}_{i,CL}}{1 + \frac{g\tilde{\gamma}_{i,CL}}{m}}} \right)$$

## 5.3 Numerical Results

Fig. 4 shows the BER performance comparison between SISO-LDM, and MRC-LDM system with  $L = 4$ . The BER performances are derived by applying (26), (27), and (28) with  $M = 2$  while both SISO-LDM and MRC-LDM transmitter send two layers of BPSK signal simultaneously with  $w = 0.3$  over the single channel, when the CL stream of mobile receiver and the EL stream of fixed receiver are transmitted over the Rayleigh fading and Nakagami- $m$  fading channel, respectively.

$$\begin{aligned}
 BER_{EL} &= BER_{CL'} \frac{P_s(E, \bar{\gamma}_{ELf})}{\log_2 M} + (1 - BER_{CL'}) \frac{P_s(E, \bar{\gamma}_{ELt})}{\log_2 M} \\
 &= \delta^{mL} \sum_{k=0}^{mL-1} \binom{mL-1+k}{k} [1-\delta]^k \cdot \frac{I_{mL} \left( \left( \frac{M-1}{M} \right) \pi; \frac{gPSK \frac{(1-\mu) \frac{E_s}{N_0}}{\rho \mu \frac{E_s}{N_0} + 1}}{m} \right)}{\log_2 M} \\
 &\quad + \left\{ 1 - \delta^{mL} \sum_{k=0}^{mL-1} \binom{mL-1+k}{k} [1-\delta]^k \right\} \cdot \frac{I_{mL} \left( \left( \frac{M-1}{M} \right) \pi; \frac{gPSK(1-\mu) \frac{E_s}{N_0}}{m} \right)}{\log_2 M}
 \end{aligned} \tag{28}$$

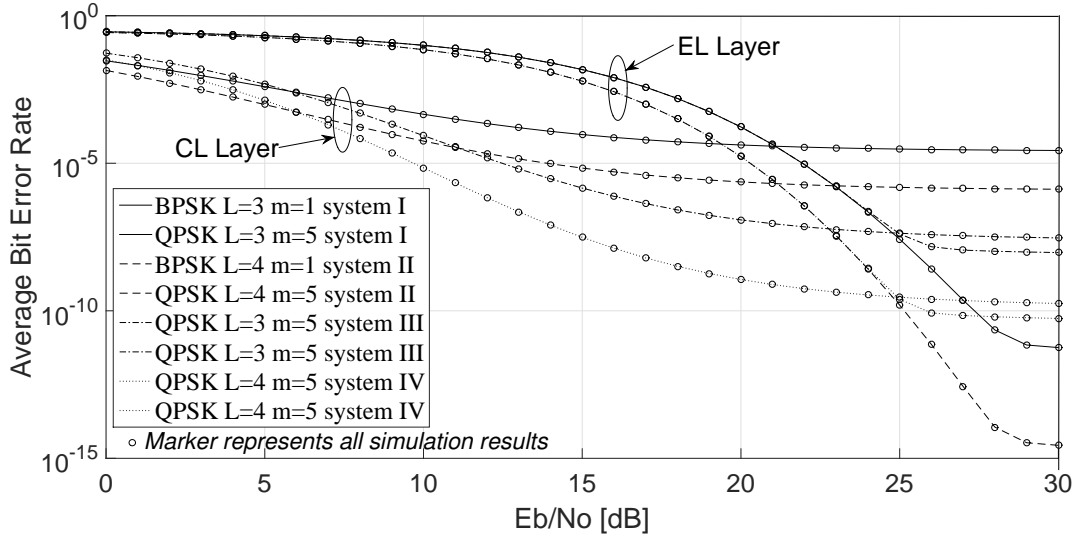


**Fig.5:** BER comparison of MRC-LDM receiver in system with  $L = 3$  versus  $L = 4$  over different fading channels.

**Table 1:** Optimum injection level in various transmission modes

System	Layer	$m, L$	Signal	Optimum point
A	CL	1,3	BPSK	$w = 0.2$ at
	EL	5,3	BPSK	BER $2 \times 10^{-5}$
B	CL	1,3	BPSK	$w = 0.26$ at
	EL	5,3	QPSK	BER $6 \times 10^{-5}$
C	CL	5,3	BPSK	$w = 0.39$ at
	EL	5,3	QPSK	BER $5 \times 10^{-7}$
D	CL	1,4	QPSK	$w = 0.23$ at
	EL	5,4	QPSK	BER $3 \times 10^{-5}$

From the figure we can see that the analysis, i.e. (27) and (28), show agreement with the simulation results. And the results show that the MRC-LDM system offers higher BER performance than SISO-LDM system clearly. Moreover, it is observed that the CL layer of SISO-LDM without channel coding (FEC) cannot apply in practice because the signal quality cannot support any wireless services, meanwhile the MRC-LDM without channel coding can increase diversity gain and can be applied in practical use. The stable BER performances of CL and EL receiver are initially occurred at  $10^{-5}$  and  $10^{-12}$  BER, respectively although the system increase transmitted power continuously. These results thus indicate that the LDM and MRC-LDM system without channel coding offer the constrained BER performance due to the presence of EP. These results agree with the author's simulations shown in Fig. 4. Fortunately, by applying channel coding in LDM system, the EP from CL layer can be perfectly cancelled [3], [6] at LDM

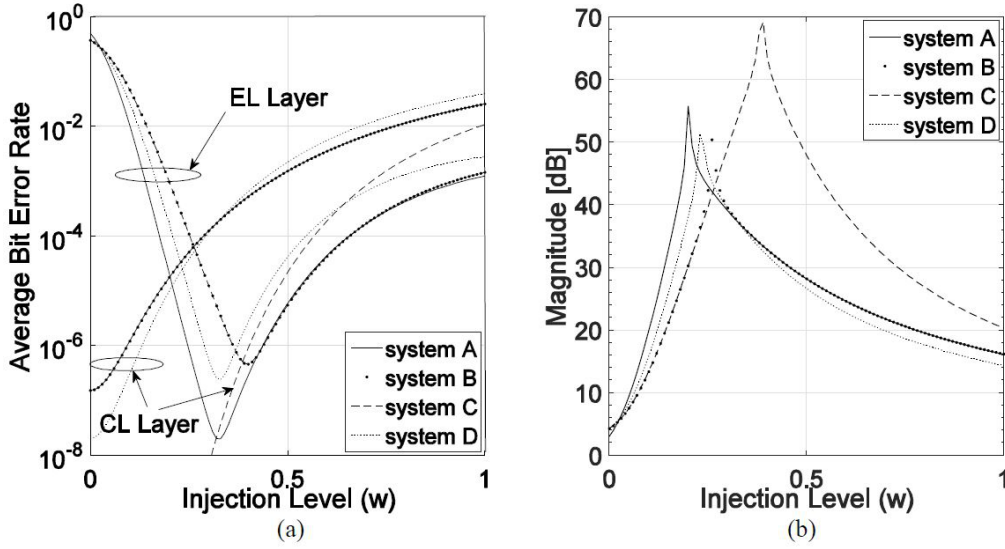
receiver.

Fig. 5 shows BER performance comparison of MRC-LDM receiver in system with  $L = 3$  versus  $L = 4$  by setting  $w = 0.24$ . The error rate performances of mobile-CL receiver ( $m = 1$ ) and fixed-CL receiver ( $m = 5$ ) are also demonstrated. These curves indicate advantage of MRC technique when increase the number of  $L$ . The stable BER performances due to the imperfect CL signal cancellation are initially occurred at 25 dB of  $E_b/N_0$ .

Again these figures demonstrate the tightness of the author's analysis, i.e. (27) and (28). By considering BERs of among CL layers, QPSK signals of system III and IV provide a higher performances than BPSK signals of system I and II because there are direct part and scattering parts at the fixed receiver of system III and IV ( $m = 4$  and  $5$ ) while the transmitted signal of system I and II are transmitted over mobile channel without a direct path ( $m = 1$ ), therefore system III and IV are slightly affected from fading channels. On the other hand, by considering BERs of among EL layers, system I and II provide higher performances than system III and IV because the mean distance ( $\Delta_s$ ) of symbol pair of BPSK signal is less than  $\Delta_s$  of symbol pair of QPSK signal. However, when focus on the mutual benefit between CL and EL layer, the results show that the performance of CL and EL layer of system IV provide the best mutual performances of  $10^{-9}$  and  $10^{-10}$  BER at 26 dB of  $E_b/N_0$ , respectively because both CL and EL receiver are fixed station and they are equipped with the maximum number of receive branches  $L$ , and these agree with the author's simulation results in Fig. 5.

Fig. 6 (a) shows the effect of injection level on the MRC-LDM system with various transmission modes





**Fig.6:** Search the optimal value of injection level.

by varying injection level and set a fixed  $E_b/N_0 = 20$  dB. There are four transmission modes in BER analysis while the transmission details and the optimum injection level of various systems can be described in Table 1. The optimum injection level in Table 1 can be searched by varying the injection level between 0 to 1 versus BER performance, and then the optimum point of injection level for CL and EL users can be chosen at the intersection point between pairs of BER curves. The results show that the optimum injection levels for system A, B, C and D are occurred at 0.2, 0.26, 0.39 and 0.23, respectively. At the optimum point of injection level, the highest mutual benefit between CL and EL layer can be acquired when the power allocation in LDM transmitter can be properly operated. For example, in system C, the optimum point of injection level is 0.39 at  $5 \times 10^{-7}$  BER while other points of injection level offer the lower mutual benefit between CL and EL layer.

Fig. 6 (b) shows the magnitude of BER distance between CL and EL layer while the BER distance can be calculated from  $10 \log_{10} |Pb_{CL} - Pb_{EL}|$ , where  $Pb_{CL}$  and  $Pb_{EL}$  denote the BER of CL and EL layer, respectively. The maximum amplitude of all curves indicate the position of the optimum injection level that offer the best mutual benefit between CL and EL layer.

## 6. CONCLUSION

A performance analysis of the MRC-LDM system over Rayleigh fading channel and Nakagami- $m$  fading channel are derived and compared with that of conventional LDM. The error rate analysis can be easily derived by calculating the MGF of the MRC-LDM SNR output which the Laplace transform can be applied to solve the complex integration. These

analysis results demonstrate that the effect of fading channel on BER performance in MRC-LDM can be mitigated by increasing the number of receive branches  $L$ . Hence the proposed system can improve the BER performance and offer the higher performance over conventional LDM. Moreover, at the optimum point of injection level, the highest mutual benefit between CL and EL layer can be acquired while the injection level controller is a necessary unit in the MRC-LDM transmitter, and the injection level should be automatically adjusted when the transmission mode and scenario are changed. In practical LDM systems [6], [7], the Ultra-High-Definition (UHD) video transmission can be operated by using high order QAM modulation with LDPC code. Thus the proposed BER analysis method need to be considered the coding gain of LDPC code and the distance of QAM symbol for computing error propagation. Furthermore, the proposed technique can be properly applied in a limited radio spectrum networks, such as cognitive radio networks or next generation wireless networks.

## 7. APPENDIX

### 7.1 Interference-plus-noise Energy of LDM System

The proposed proofs in this appendix are derived to present the interference-plus-noise energy of CL and EL layers in LDM system.

$$\begin{aligned}
 & 1) \text{ Appendix 1 : Proof of (5) :} \\
 E[\tilde{n}_i \tilde{n}_i^*] &= E \left[ (wS_2^{(d)} + h_i^{-1}n_i) \times (wS_2^{(d)} + h_i^{-1}n_i)^* \right] \\
 &= w^2 E \left[ |S_2^{(d)}|^2 \right] + wE \left[ S_2^{(d)} \frac{n_i^*}{h_i} \right] + wE \left[ S_2^{(d)*} \frac{n_i}{h_i} \right] +
 \end{aligned}$$

$$N_0 E \left[ \frac{1}{|h_i|^2} \right] \\ = w^2 E_p + N_0 = w^2 \frac{E_s}{(1+w^2)} + N_0$$

2) *Appendix 2 : Proof of interference – plus – noise energy for (10) :*

$$E[n\hat{n}^*] = E \left[ \left( \frac{h_i^{-1}}{w} n_i \right) \times \left( \frac{h_i^{-1}}{w} n_i \right)^* \right] \\ = \frac{N_0}{w^2 |h_i|^2} = \frac{N_0}{w^2}$$

3) *Appendix 3 : Proof of interference – plus – noise energy for (13) :*

$$E[n''n''^*] = E \left[ \left( \frac{\Delta_s}{w} + n \right) \times \left( \frac{\Delta_s}{w} + n \right)^* \right] \\ = E \left[ \left( \frac{\Delta_s}{w} + \frac{h_i^{-1}}{w} n_i \right) \times \left( \frac{\Delta_s}{w} + \frac{h_i^{-1}}{w} n_i \right)^* \right] \\ = \frac{1}{w^2} E[|\Delta_s|^2] + \frac{1}{w^2} E \left[ \frac{\Delta_s n_i^*}{h_i^*} \right] + \frac{1}{w^2} E \left[ \frac{\Delta_s n_i}{h_i} \right] + \frac{N_0}{w^2} E \left[ \frac{1}{|h_i|^2} \right] \\ = \frac{\rho}{w^2} E[|S|^2] + \frac{N_0}{w^2} E \left[ \frac{1}{|h_i|^2} \right] = \frac{\rho E_p}{w^2} + \frac{N_0}{w^2} \\ = \frac{1}{w^2} \left( \frac{\rho E_s}{(1+w^2)} + N_0 \right)$$

## 7.2 MGF of Rayleigh and Nakagami- $m$ Distribution

This appendix derives MGF of Rayleigh and Nakagami- $m$  distribution as follows.

1) *Appendix 4 : Proof of MGF in (18) and (23) :*

$$M_r \left( -\frac{g}{\sin^2 \phi}, \bar{\gamma} \right) = \int_0^\infty \frac{1}{\bar{\gamma}} e^{-\frac{\gamma}{\bar{\gamma}}} \cdot e^{-\frac{g\gamma}{\sin^2 \phi}} d\gamma \\ = \int_0^\infty \frac{1}{\bar{\gamma}} e^{-\frac{\gamma}{\bar{\gamma}} - \frac{g\gamma}{\sin^2 \phi}} d\gamma = \frac{1}{\bar{\gamma}} \int_0^\infty e^{-\gamma \left( \frac{1}{\bar{\gamma}} + \frac{g}{\sin^2 \phi} \right)} d\gamma$$

By applying Laplace transform, we know that  $\int_0^\infty e^{-st} dt = \frac{1}{s}$ . Thus the MGF of Rayleigh distribution can be written as

$$M_r \left( -\frac{g}{\sin^2 \phi}, \bar{\gamma} \right) = \frac{1}{\bar{\gamma}} \left( \frac{1}{\bar{\gamma}} + \frac{g}{\sin^2 \phi} \right)^{-1} = \frac{\sin^2 \phi}{\sin^2 \phi + g\bar{\gamma}}$$

2) *Appendix 5 : Proof of MGF in (20) and (24) :*

$$M_m \left( -\frac{g}{\sin^2 \phi}, \bar{\gamma} \right) = \int_0^\infty e^{-\frac{g\gamma}{\sin^2 \phi}} \cdot \frac{m^m \gamma^{m-1}}{\bar{\gamma}^m \Gamma(m)} e^{-\frac{\gamma}{\bar{\gamma}}} d\gamma \\ = \frac{m^m}{\bar{\gamma}^m \Gamma(m)} \int_0^\infty \gamma^{m-1} \cdot e^{-\gamma \left( \frac{m}{\bar{\gamma}} + \frac{g}{\sin^2 \phi} \right)} d\gamma$$

By applying Laplace transform, we know that  $\int_0^\infty t^P e^{-st} dt = \frac{\Gamma(P+1)}{s^{P+1}}$ , where  $s > 0$ ,  $P > -1$ . Thus the MGF of Nakagami- $m$  distribution can be written as

$$M_m \left( -\frac{g}{\sin^2 \phi}, \bar{\gamma} \right) = \frac{m^m}{\bar{\gamma}^m \Gamma(m)} \cdot \frac{\Gamma(m-1+1)}{\left( \frac{m}{\bar{\gamma}} + \frac{g}{\sin^2 \phi} \right)^{m-1+1}}$$

$$= \frac{m^m}{\bar{\gamma}^m} \left( \frac{m}{\bar{\gamma}} + \frac{g}{\sin^2 \phi} \right)^{-m} = \left( \frac{\sin^2 \phi}{\sin^2 \phi + \frac{g\bar{\gamma}}{m}} \right)^m$$

## References

- [1] N. Loghin et al., "ATSC 3.0 physical layer specification: An overview," *IEEE Trans. Broadcast*, Vol. 62, No. 1, pp.159-171, 2016.
- [2] E. Garro et al., "Layered Division Multiplexing With Multi-Radio-Frequency Channel Technologies," *IEEE Trans. Broadcast*, Vol. 62, No. 2, pp.365-374, 2016.
- [3] Y. Wu, B. Rong, K. Salehian and G. Gagnon, "Cloud transmission: A new spectrum-reuse friendly digital terrestrial broadcasting transmission system," *IEEE Trans. Broadcast*, Vol. 58, No. 3, pp.329-337, 2012.
- [4] S. Cho et al., "Low-Complexity Decoding Algorithms for the LDM Core Layer at Fixed Receivers in ATSC 3.0," *IEEE Trans. Broadcast*, Vol. 63, No. 1, pp. 293-303, 2017.
- [5] W. Li et al., "Using LDM to Achieve Seamless Local Service Insertion and Local Program Coverage in SFN Environment," *IEEE Trans. Broadcast*, Vol. 63, No. 1, pp. 250-258, 2017.
- [6] S. -I. Park et al., "Low Complexity Layered Division Multiplexing for ATSC 3.0," *IEEE Trans. Broadcast*, 2016, 62, (1), pp. 233-243.
- [7] L. Zhang et al., "Layered-Division-Multiplexing: Theory and Practice," *IEEE Trans. Broadcast*, Vol. 62, No. 1, pp. 216-230, 2016.
- [8] L. Zhang et al., "Capacity Analysis of LDM-Based DTV System with Flexible MIMO Configuration," *Proc. IEEE Int. Conf. Broadband Multimedia Syst. Broadcasting*, pp. 1-7, 2016.
- [9] X. Zhu, Z. Wang and J. Cao, "NOMA-Based Spatial Modulation," *IEEE Access*, Vol. 5, pp. 3790-3800, 2017.
- [10] L. Zhang et al., "Improving LTE eMBMS with Extended OFDM Parameters and," *IEEE Trans. Broadcast*, Vol. 63, No. 1, pp. 33-47, 2017.
- [11] R. S. Rabaca et al., "Implementation of LDM/ISDB-T broadcast system using diversity at reception," *Proc. IEEE Int. Conf. Broadband Multimedia Syst. Broadcasting*, pp. 1-4, 2017.
- [12] J. Montalban et al., "Error Propagation in the Cancellation Stage for a Multi-Layer Signal Reception," *Proc. IEEE Int. Conf. Broadband Multimedia Syst. Broadcasting*, pp. 1-5, 2014.
- [13] M. A. S. Alouini and A. J. Goldsmith, "A Unified Approach for Calculating Error Rates of Linearly Modulated Signals over Generalized Fading Channels," *IEEE Trans. Commun.*, Vol. 47, No. 9, pp. 1324-1334, 1999.
- [14] M. S. Alouini and M. K. Simon, "An MGF-Based Performance Analysis of Generalized Selection Combining over Rayleigh Fading Channels," *IEEE Trans. Commun.*, Vol. 48, No. 3, pp. 401-415, 1999.

- [15] S. Mumtaz, J. Rodriguez and L. Dai, "mmWave Massive MIMO A Paradigm for 5G," *Academic Press*, 2016.
- [16] S. I. Park et al., "Field Test Results of Layered Division Multiplexing for the Next Generation DTV System," *IEEE Trans. Broadcast*, Vol. 63, No. 1, pp. 260-266, 2017.
- [17] A. Goldsmith, *Wireless Communications*, Cambridge University Press, 2005.
- [18] G. L. Stuber, *Principles of Mobile Communication*, Kluwer Academic Publishers, 2002.
- [19] J. W. Craig, "A new, simple, and exact result for calculating the probability of error for two-dimensional signal constellations," *Proc. IEEE Int. Conf. Military Commun.*, pp. 571-575, 1991.
- [20] J. G. Proakis, *Digital Communications*, McGraw Hill, 1989.



**Tanapong Khumyat** was born in Tak, Thailand, in 1978. He received Ph.D. degree in March 2014 from Suranaree University of Technology. His Ph.D. research was concerned with MIMO communication systems. He is currently lecturer in Department of Electrical Engineering at the Rajamangala University of Technology Lanna Tak. His research area concerns wireless communication systems.